structurally characterized, while only two Ti complexes are known. Structures of molybdenum (pyrazolyl)borates, include complexes of Mo(II), -(III), -(IV), -(V), -(VI), and -(VII). They show the expected general trend of shorter Mo-N bond distances with increasing oxidation state, ranging from ~2.21 Å for Mo(II) to ~2.16 Å for Mo(VII). The Ti complexes, both reported as Ti(III), have M-N values averaging 2.18 Å. The V(III)-N bond lengths observed in II and VI average 2.12 Å, and the V(IV)-N bond lengths in III and V, 2.11 Å. Since the M(III) ionic radii for Mo, Ti, and V are expected to be roughly similar (0.65, 0.67, and 0.64 Å, respectively),[35] a comparison of the structures with this oxidation state suggests that the vanadium is bound somewhat more tightly to the ligand than either Ti or Mo although these differences are small.

It is interesting to compare directly the analogous {HB(Me$_2$pz)$_3$}MCl$_2$(Me$_2$pz) structures for V(III) and Ti(III). These two complexes differ only by the fact that the V(III) complex is cationic and isolated as the potassium salt, whereas the Ti(III) species is neutral.[33] This implies that the free pyrazole is bound as a pyrazolide anion in the V(III) complex and as a neutral protonated pyrazole with the Ti. The X-ray structure reveals that the coordinated pyrazolide in the V(III) complex has a totally delocalized structure, as was expected. A neutral protonated pyrazole should have a localized structure with alternating C-C bond lengths. Indeed, the Ti(III) complex shows evidence of some electronic localization, which is consistent with its formulation as a coordinated neutral molecule.

Summary. Vanadium(III) and -(IV) complexes of the 3,5-dimethyl-substituted tris(pyrazolyl)borate ligand have been prepared and characterized by X-ray crystallography. The ligand is found to exhibit both bi- and tridentate coordination modes that are solvent dependent. These complexes may be useful as models for vanadium-histidine binding in metalloproteins. Study of the substitution chemistry of these complexes, particularly with peroxides, is underway and will be reported elsewhere.

Acknowledgment. We wish to thank Professors Alan Cowley and Richard Jones, The University of Texas at Austin, for the use of their diffractometer. We also thank Prof. John Hubbard for assistance with collection of X-ray data at The University of Vermont.

Supplementary Material Available: Tables of bond lengths, bond angles, H atom coordinates and isotropic displacement parameters, and anisotropic displacement parameters (20 pages); listings of observed and calculated structure factors (60 pages). Ordering information is given on any current masthead page.

Contribution from the Department of Chemistry, University of California, Berkeley, California 94720

Synthesis and Characterization of Vanadium(V) and -(IV) Hydroxamate Complexes. X-ray Crystal Structures of Oxochlorobis(benzohydroxamato)vanadium(V) and Oxoisopropoxo(*N*,*N*′-dihydroxy-*N*,*N*′-diisopropylheptanediamido)vanadium(V)

Diane C. Fisher, Susan J. Barclay-Peet, Carol A. Balfe, and Kenneth N. Raymond*

Received September 14, 1988

Although hydroxamic acids have been used for many years in colorimetric analyses of vanadium, the full characterization of the complexes formed has not been accomplished. In this study a number of vanadyl dihydroxamate complexes are described. Two vanadium(V) complexes, oxochlorobis(benzohydroxamato)vanadium(V) (VOCl(bz)$_2$) and oxoisopropoxo(*N*,*N*′-dihydroxy-*N*,*N*′-diisopropylheptanediamido)vanadium(V) (VO(OiPr)L), are structurally characterized by X-ray crystallography, and both have pseudooctahedral coordination sites in which the second monodentate group is cis to the oxo oxygen. Large, opaque, purple-black crystals of VOCl(bz)$_2$ were found to conform to monoclinic space group $P2_1/n$, with a = 11.1054 (15) Å, b = 10.853 (16) Å, c = 18.3508 (22) Å, and β = 94.92 (1)°. The measured (1.40 g cm^{-3}) and calculated (1.40 g cm^{-3}) densities are consistent with 4 molecules of VOCl(bz)$_2$/unit cell. Least-squares refinement of the structure converged with conventional (and weighted) R indices (on $|F_o|$) of 3.43% (4.76%) with the use of 2795 reflections with $F_o^2 > 3\sigma(F_o^2)$. Crystals of VO(OiPr)L were obtained as orange-red hexagonal prisms; they conform to space group $P2_1/c$, with a = 8.2170 (10) Å, b = 15.7946 (15) Å, c = 16.2124 (19) Å, and β = 97.48 (1)°. The measured (1.28 g cm^{-3}) and calculated (1.28 g cm^{-3}) densities indicate 2 molecules of the centrosymmetric dimer [VO(OiPr)L]$_2$/unit cell. Least-squares refinement of the structure converged with conventional (and weighted) R indices of 5.05% (6.19%) with use of 1489 reflections with $F_o^2 > 3\sigma(F_o^2)$. These are the first X-ray crystallographically determined structures of any vanadium hydroxamate complexes. It is found that under some experimental conditions tris(hydroxamato)vanadium(IV) complexes are formed, resulting from the highly unusual dissociation of the vanadyl V=O bond; these undergo reversible electrochemical reduction to the corresponding vanadium(III) complexes. Both dihydroxamic acid and monohydroxamic acid ligand complexes are characterized, and their vis/UV spectra and other physical properties are described.

Introduction

Hydroxamic acids form highly colored complexes with vanadium(V) or -(IV) under a wide variety of conditions and have been used extensively as analytical reagents for the detection of this metal.[1-8] Nevertheless, very little is known about the structure of the complexes that are formed. The most commonly used analytical procedure is the extraction of vanadium(V) by hydroxamic acids from aqueous HCl into an organic phase (usually chloroform), and spectrophotometric detection of the intensely purple-black species (λ_{max} = 510-575 nm, ϵ = 3.9-6.9 × 10^3 cm^{-1} M^{-1}) which form. Although this reaction has been used analytically for over 30 years,[8] it was not until relatively recently that the colored species was identified as oxochlorobis(hydroxamato)vanadium(V), when Pande and Tandon succeeded in isolating oxochlorobis(*N*-phenylbenzohydroxamato)vanadium(V).[9] This and similar compounds are formed under highly acidic conditions (3-8 N HCl), where some potentially interfering metals (such as iron) do not form hydroxamate complexes.[4] Selectivity can be further enhanced by varying the functionalities attached to the hydroxamate moieties.[4] Because of this selectivity, and the fact

* To whom correspondence should be addressed.

(1) Agrawal, Y. K.; Mehd, G. D. *Int. J. Environ. Anal. Chem.* **1981**, *10*, 183-188.
(2) Agrawal, Y. K. *Bull. Soc. Chim. Belg.* **1980**, *89*, 261-265.
(3) Nanewar, R. R.; Tandon, U. *Talanta* **1978**, *25*, 352-354.
(4) Bhura, D. C.; Tandon, S. G. *Anal. Chim. Acta* **1971**, *53*, 379-386.
(5) Tandon, S. G.; Bhattacharya, S. C. *J. Ind. Chem. Soc.* **1970**, *47*, 583-589.
(6) Cassidy, R. M.; Ryan, D. E. *Can. J. Chem.* **1968**, *46*, 327-330.
(7) Ryan, D. E. *Analyst* **1960**, *85*, 569-574.
(8) Lutwick, G. D.; Ryan, D. E. *Can. J. Chem.* **1954**, *32*, 949-955.
(9) Pande, K. R.; Tandon, S. G. *J. Inorg. Nucl. Chem.* **1980**, *42*, 1509.

0020-1669/89/1328-4399$01.50/0

Table I. Analytical Data for VO(hydroxamate)$_2$(alkoxide) Complexes[a]

				UV/vis data,[b]	elemental anal., % found (% calcd)			
n	R	mp, °C	IR data, cm^{-1}	λ_{max} (ϵ)	C	H	N	V
3	CH_3	190 dec	2789 (m, C-H, OCH_3), 1561, 1576 (s, C=O), 958 (s, V=O)	272 (3600), 446 (3020)	42.47 (42.11)	6.67 (6.77)	8.25 (8.19)	16.1 (14.9)
3	C_2H_5	186 dec	1560, 1575 (s, C=O), 952 (s, V=O)		43.75 (43.82)	7.10 (7.07)	7.82 (7.86)	
5	CH_3	169 dec	2797 (m, C-H, OCH_3), 1570 (b, s, (C=O), 953 (s, V=O)	272 (3600), 446 (3290)	45.59 (45.41)	7.29 (7.35)	7.63 (7.57)	
5	C_2H_5	166 dec	1562 (b, s, C=O), 953 (s, V=O)		47.10 (46.87)	7.67 (7.61)	7.18 (7.29)	14.3 (13.3)
10	CH_3	164 dec	2798 (m, C-H, OCH_3), 1563 (s, b, C=O), 955 (s, V=O)	272 (3700), 446 (3340)	51.68 (51.81)	8.20 (8.47)	6.36 (6.36)	12.4 (11.6)

[a] The dihydroxamate ligands (with *n* methylene groups) are shown in Figure 1b. The alkoxide ligand is OR. [b] λ_{max} in nanometers.

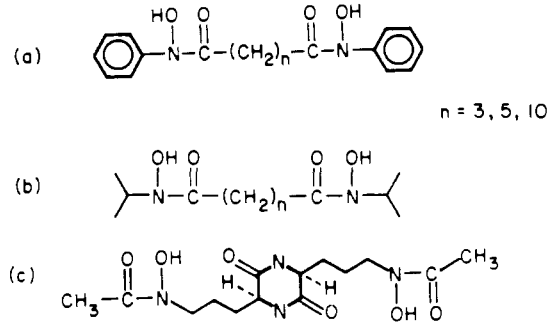

Figure 1. Ligands that have been used to prepare vanadium dihydroxamate complexes: (a) *N*-phenyl dihydroxamic acids; (b) *N*-isopropyl derivatives used in the current study; (c) the naturally occurring dihydroxamic acid, rhodotorulic acid.

that they are detectable in trace quantities, these compounds have found widespread use in vanadium detection.

Oxo chloro bis(hydroxamato) complexes have been found to turn red-orange when small amounts of alcohol are present.[9,10] This red-orange species has been identified as oxoalkoxobis(hydroxamato)vanadium(V). These complexes can be synthesized in a direct manner or via the oxo hydroxo derivatives and have been used both in the detection of vanadium and of alcohols.[10]

Previous workers found[11] that alkoxo complexes were isolated only when there was an electron-withdrawing group present on the aromatic ring of the hydroxamate ligand. From this observation it was postulated that the OH proton in the vanadium(V) complex must be slightly acidic in order for the alkoxo complex to form. The oxohydroxovanadium(V) complexes of several *N*-phenyl dihydroxamate ligands (see Figure 1a) have been reported[12-14] for $n = 2-5$ methylene units separating the hydroxamate functional groups. The compounds were characterized as $VO(OH)(LH)_2$ ($n = 2$), $VO_2(LH)\cdot 3H_2O$ ($n = 3$), VO(OH)L ($n = 4$), and $[VO(OH)]_3L_2(OH)_2$ ($n = 5$) on the basis of elemental analyses; no further characterization has been reported.

Because there is a lack of detailed structural information on these analytically useful complexes, and because of a general interest in metal hydroxamate complexes, both oxochlorobis(benzohydroxamato)vanadium(V) and the oxoisopropoxobis(hydroxamato)vanadium(V) complex of the ligand in Figure 1b (with $n = 5$) have been crystallized and structurally characterized. Preliminary characterization of some vanadium(IV) complexes of the dihydroxamate ligand with $n = 3$ (Figure 1b) and the dihydroxamate siderophore, rhodotorulic acid anion (RA, Figure 1c) is also reported.

Experimental Section

Physical Properties. Visible spectra were recorded on a HP 8450A UV/vis spectrophotometer. IR spectra were recorded from KBr pellets on either a Perkin-Elmer 597 IR spectrometer or a Nicolet 5DXE FTIR spectrometer. NMR spectra ($CDCl_3$/TMS) were recorded with either a 200- or 250-MHz Fourier transform spectrometer. Melting points were taken in open capillaries with a Mel-temp apparatus and are uncorrected. EPR data on methanol or 1:1 chloroform/toluene samples in quartz tubes were obtained at X-band frequencies at 110 K and at room temperature by using a Varian E-3 spectrometer. Molecular weight measurements were made by using gel partition chromatography on a Sephadex LH-20 column (30.5-cm length, 2-cm diameter) with methanol/chloroform (1:1) as the eluting solvent. The dihydroxamic acid ligands were synthesized by literature methods,[15] as was benzohydroxamic acid[16] (the anion is abbreviated as bz) and vanadyl acetylacetonate[17] (the anion is abbreviated as acac). All other starting materials and solvents were reagent grade and were used without further purification. Cyclic voltammetry experiments were performed by using the PAR Model 173 potentiostat/galvanostat interfaced with a Model 179 digital coulometer, a Model 178 electrometer probe (to monitor the potential between the working and reference electrodes), and a Model 175 universal programmer (to generate the wave form). The three-electrode cell was fitted with a Pt working electrode obtained from Bioanalytical Systems, Bloomington, IN, a Pt wire counter electrode, and a $Ag/AgNO_3$ (0.01 M), TEAP (0.1 M), DMSO reference electrode placed in a Luggin probe. The reference electrode was calibrated vs the ferrocene/ferrocenium couple in DMSO.

In addition to standard voltammograms, electrochemical data were recorded in the semiderivative mode. A semiderivative circuit was inserted in series between the voltage output of the current-follower and the *y* axis of the recording device. A toggle switch allowed alternate recording of standard *i*–*E* curves. For scan rates $v \leq 200$ mV/s, a Hewlett-Packard Model 7040A XY recorder was used. A Tektronix Type 549 storage oscilloscope with a Type 1A1 dual plug-in unit was fitted with an Oscillotron MII camera and was used to record scans at rates $v \geq 500$ mV/s.

The analog circuit used for transforming the *i*–*E* curve of cyclic voltammetry to the e–*E* curve of semiderivative voltammetry was based on those described by Oldham.[18,19] [The semiintegrating circuit used was that shown in Figure 10 of ref 18; there is a resistor that is incorrectly labeled as 830 kΩ; the correct value is 8300 kΩ.[19]] The semidifferentiator was built by using the circuit shown in circuit B of Figure 4 in ref 19. A CA3140T operational amplifier and a 15-V power supply were used.[20]

Spectroelectrochemical data were recorded with an optically transparent thin-layer electrode (OTTLE).[21] The OTTLE cell used here is a sandwich cell based on the design reported by Bowden and Hawk-

(10) Sahu, B. R.; Tandon, U. *J. Ind. Chem. Soc.* **1983**, *60*, 615–616.
(11) Dutta, R. L.; Ghosh, S. J. *J. Ind. Chem. Soc.* **1967**, *44*, 369–376.
(12) Ghosh, N. N.; Sarkar, D. K. *J. Ind. Chem. Soc.* **1970**, *47*, 562–566.
(13) Ghosh, N. N.; Sarkar, D. K. *J. Ind. Chem. Soc.* **1969**, *46*, 528–530.
(14) Ghosh, N. N.; Sarkar, D. K. *J. Ind. Chem. Soc.* **1968**, *45*, 550–581.
(15) Smith, W. L.; Raymond, K. N. *J. Am. Chem. Soc.* **1980**, *102*, 1252–1255.
(16) Blatt, A. H. *Organic Syntheses*; Wiley: New York, 1943; Collect Vol. II, pp 67–68.
(17) Rowe, R. A.; Jones, M. M. *Inorg. Synth.* **1957**, *5*, 113–116.
(18) Oldham, K. B. *Anal. Chem.* **1973**, *45*, 39–47.
(19) Dalrymple-Alford, P.; Goto, M.; Oldham, K. B. *Anal. Chem.* **1977**, *49*, 1390–1394. For additional details of the cells and circuitry used, see: Carol A. Balfe, Carol A. Ph.D. Thesis, UC Berkeley, 1984.
(20) A comment on the output obtained by using this particular circuit is in order here. The output of the semidifferentiating circuit is given by[19] $V_{out} = -(2.00\ s^{1/2})d^{1/2}/dt^{1/2}$. Hence, the effect of the circuit is to multiply the sensitivity setting of the PAR 13 potentiostat by a factor of 0.5 $s^{-1/2}$ and to change the sign of the current axis. All semiderivative voltammograms in the supplementary material are scaled to the correct current output and use the sign convention just described. The accuracy of the semiderivative circuit was verified by using a solution that was 1 mM in Cu^{2+}, Pb^{2+}, Cd^{2+}, and Zn^{2+} with 0.1 M KNO_3 as electrolyte. When a hanging mercury drop electrode of known surface area was used, semiderivative voltammograms at 200, 100, 50 and 20 mV·s^{-1} were recorded. The peak heights, peak widths, and relative peak potentials were measured and were found to agree, within experimental error, with the values predicted by theory. Likewise, a plot of e_p vs v, the scan rate, was found to be linear as predicted. Similar results were obtained for the ferrocene/ferrocenium couple in acetonitrile.
(21) Murray, R. W.; Heineman, W. R.; O-Dom, G. W. *Anal. Chem.* **1967**, *13*, 1666–1668.

ridge.[22] The only modifications of that design are that the ports for the Hamilton valves were machined as an integral part of the cell body, rather than being cemented on, and the port for the filling valve was placed on the side rather than in front.

Spectroelectrochemical experiments were performed for three different solutions of vanadium(IV) rhodotorulic acid complexes at pH 3.0, all of which gave the same results (Figure S1).[23] The solutions examined were (1) H_2RA and $VOSO_4$ (1:1) under anaerobic conditions, (2) H_2RA and $VOSO_4$ (1:1) in a solution that was first exposed to air, and (3) NH_4VO_3 and H_2RA (1:1) under anaerobic conditions. Repeated cyclic potential sweeps were done between −0.15 and 0.90 V. For each cycle the reduced species was colorless, having no absorption bands in the visible region, while the oxidized species was purple, having a spectrum identical with that of the purple solution described previously. Integration of the i–E curve (inset Figure S1) verified that a one-electron transfer was involved. The same pattern of spectral changes was observed for the air oxidation of a solution of $VOSO_4$ and H_2RA (1:1).

Preparation of Compounds. VO(hydroxamate)$_2$(alkoxide) Complexes. These were prepared by reaction of stoichiometric amounts (1:1) of vanadyl acetylacetonate and the dihydroxamate ligand (n = 3, 5, 10) in the appropriate alcohol under air. The solutions rapidly became red and were boiled at reflux for 2 h to ensure complete formation of the hydroxamate complexes. The n = 5 and 10 complexes were isolated as crystalline and microcrystalline complexes by evaporation of the alcoholic solutions at room temperature. The n = 3 complex precipitated as a red powder from the refluxing alcoholic solutions and was not further purified. Oxidation of vanadium from the +4 to the +5 state occurs during the reaction, as evidenced by the fact that all of the complexes yield sharp, well-resolved NMR spectra with no paramagnetic shifts or broadening. X-ray-quality crystals of oxoisopropoxo(*N*,*N*′-diisopropylheptanediamido)vanadium(V) [VO(OiPr)L (n = 5)] were obtained by briefly heating the crystals from the first evaporation in more 2-propanol to redissolve them, followed by a second slow evaporation. Analytical data for all of the complexes are shown in Table I.

VO(bz)$_2$Cl. Oxochlorobis(benzohydroxamato)vanadium(V) was synthesized by a modification of the procedure that Pande and Tandon used to make the analogous *N*-phenylbenzohydroxamato compound.[9] Benzohydroxamic acid (300 mg) was dissolved in 30 mL of ethyl acetate. This solution was shaken with 50 mL of a saturated aqueous solution of ammonium metavanadate and 25 mL of concentrated HCl. The resultant mixture immediately turned very deep purple, with most of the color in the organic phase but a significant amount in the aqueous phase. The phases were separated and the aqueous phase was extracted with 30 mL of ethyl acetate (EtOAc). The EtOAc fractions were combined and shaken a second time with fresh ammonium metavanadate and HCl, to ensure complete reaction. The aqueous phase was again washed with EtOAc. The combined organic fractions were dried over anhydrous $MgSO_4$. This solution was then carefully added to a flask beneath a layer of *n*-hexane, and the two solvents were allowed to mix by slow diffusion. Large, opaque, purple-black crystals of VOCl(bz)$_2$·EtOAc were deposited and found to be suitable for X-ray diffraction. Anal. Found (calcd) for $C_{18}H_{20}N_2O_7VCl$: C, 46.47 (46.72); H, 4.29 (4.36); N, 6.11 (6.05); V, 12.0 (11.01); Cl, 8.20 (7.66). Note: the sample exploded during chloride analysis.

Preparation of Vanadium(IV) Complexes. All procedures were carried out under an argon atmosphere by using inert-atmosphere techniques.

VO(RA)·H$_2$O (Oxovanadium(IV) Rhodotorulate Hydrate). (a) From H$_2$O. Oxovanadium(IV) sulfate (60 mg, 0.300 mmol) was dissolved in water, and the solution was degassed by freeze–pump–thaw cycles and added to an aqueous slurry of rhodotorulic acid (105 mg, 0.31 mmol) (see Figure 1c), which had also been degassed. As the rhodotorulic acid slowly dissolved, the resultant solution turned deep red-violet and was concentrated under reduced pressure until a pale violet precipitate appeared; this was removed by filtration after 24 h, washed successively with ethanol and diethyl ether, and dried in vacuo. Yield: 35 mg (32%). The UV/vis spectrum of the filtrate was characterized by an absorption maximum at 516 nm and a shoulder at 390 nm. Anal. Found (calcd) for $C_{14}H_{22}N_4O_7V·H_2O$: C, 39.34 (39.54); H, 5.47 (5.22); N, 12.81 (13.17). **(b) From Methanol.** Essentially the same procedure as that in water was followed with the substitution of VO(acac)$_2$ as the starting material (80 mg, 0.30 mmol). As the ligand slowly dissolved with mixing of the two solutions, the solution became colorless. This was followed by slow precipitation of a violet powder. Yield: 40 mg (40%).

Vanadium(IV) Tris(hydroxamate) Rhodotorulate Complex. An aqueous slurry of oxovanadium(IV) sulfate (54 mg, 0.27 mmol) was degassed and added to a slurry of rhodotorulic acid (188 mg, 0.55 mmol).

Table II. Crystallographic Summary

	VOCl(bz)$_2$	VO(OiPr)L
mol formula	$C_{14}H_{12}ClN_2O_5V·CH_3COOC_2H_5$	$[C_{16}H_{31}N_2O_6V]_2$
fw	462.76	796.74
space group	$P2_1/n$ (No. 14)	$P2_1/c$ (No. 14)
a, Å	11.1054 (15)	8.2170 (10)
b, Å	10.8535 (16)	15.7946 (15)
c, Å	18.3508 (22)	16.2124 (19)
β, deg	94.92 (1)	97.48 (1)
V, Å^3	2203.7 (8)	2086.2 (7)
formula units/cell	4	2
d_{obsd}, g cm^{-3}	1.40	1.28
d_{calcd}, g cm^{-3}	1.40	1.28
R, %	3.43	5.05
R_w, %	4.76	6.19
λ, Å	0.71073	0.71073
μ, cm^{-1}	5.94	5.41
abs transm coeff	0.8429–0.9373	0.9905–0.9998

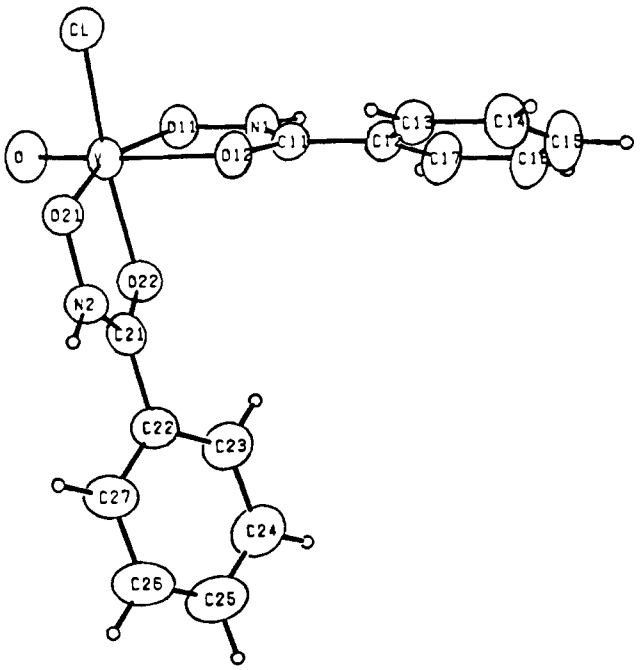

Figure 2. Labeling diagram for oxochlorobis(benzohydroxamato)vanadium(V).

A deep burgundy red color appeared as both the starting materials slowly dissolved. Reducing the volume did not yield a precipitate. The UV/vis spectrum gave absorption maxima at 390 and 516 nm ($\epsilon \approx 2 \times 10^3$ M^{-1} cm^{-1}). Addition of a solution of sodium tetraphenylborate produced a dark red-violet powder. Elemental analysis was not definitive (C, H, N, V) but gave a RA:V ligand to metal ratio of 3:2.2 based on the N:V ratio.

X-ray Diffraction Studies. Crystallographic data for VOCl(bz)$_2$ and VO(OiPr)L are summarized in Table II. Preliminary precession photography uniquely determined the space group of both crystals to be $P2_1/c$. The alternate setting of $P2_1/n$ was used for VOCl(bz)$_2$ to give a less oblique cell. Diffraction data on the crystals mounted on glass fibers were collected with an Enraf-Nonius CAD-4 diffractometer by the θ–2θ scan technique. The cell dimensions and orientation matrices were determined on the diffractometer as previously described.[24] Accurate cell dimensions were derived from least-squares refinement of the setting angles of 24 high-angle reflections. Three high-angle reflections were checked every 200 reflections as orientation standards, and three strong reflections were checked every 1 h as intensity standards. No decay of intensity was observed for either crystal. The VOCl(bz)$_2$ crystal had very well formed, easily indexed faces. An absorption correction was therefore applied to the data on the basis of the known crystal dimensions and known absorptivity of the contents. An empirical absorption correction based on ψ scans was applied to VO(OiPr)L (n = 5). After deletion of systematically absent reflections and averaging of equivalent reflections,

(22) Hawkridge, F. M. *Bowden, E. F. J. Electroanal. Chem. Interfacial Electrochem.* **1981**, *125*, 367–386.
(23) See paragraph at end of paper regarding supplementary material.
(24) Freyberg, D. P.; Robbins, J. L.; Raymond, K. N.; Smart, J. C. *J. Am. Chem. Soc.* **1979**, *101*, 892–897.

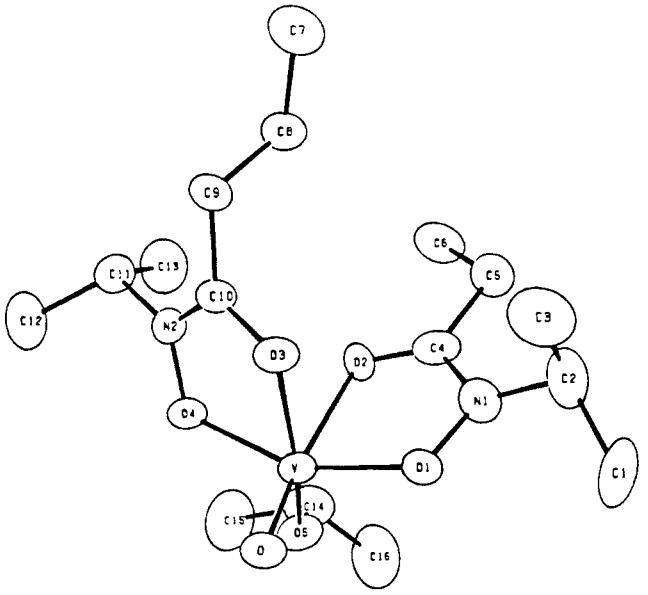

Figure 3. Labeling diagram for VO(OiPr)L (n = 5), showing half of the centrosymmetric dimer.

Table III. Positional Parameters and Anisotropic Thermal Parameters for $VOCl(bz)_2$

atom	x	y	z	B_{eqv}, Å^2
V	0.11890 (4)	0.32601 (4)	0.29526 (3)	3.333 (9)
Cl	0.04249 (7)	0.41705 (7)	0.18946 (4)	4.55 (2)
O	0.0008 (2)	0.2534 (2)	0.3152 (1)	4.87 (5)
O11	0.1914 (2)	0.1853 (2)	0.2624 (1)	3.65 (4)
O12	0.2936 (2)	0.3904 (2)	0.2627 (1)	3.61 (4)
O21	0.1059 (2)	0.4901 (2)	0.33751 (9)	3.35 (4)
O22	0.2181 (2)	0.3081 (2)	0.3916 (1)	3.88 (4)
O31	0.3093 (2)	0.2481 (2)	0.0584 (1)	5.32 (5)
O32	0.3640 (3)	0.4313 (2)	0.0210 (2)	8.60 (7)
N1	0.3068 (2)	0.1905 (2)	0.2452 (1)	3.64 (5)
N2	0.1756 (2)	0.5047 (2)	0.4028 (1)	3.58 (5)
C11	0.3567 (2)	0.3028 (2)	0.2455 (1)	3.23 (5)
C12	0.4821 (2)	0.3168 (3)	0.2250 (2)	3.56 (6)
C13	0.5144 (3)	0.4310 (3)	0.1993 (2)	4.16 (6)
C14	0.6316 (3)	0.4504 (3)	0.1802 (2)	5.56 (8)
C15	0.7150 (3)	0.3560 (4)	0.1888 (2)	6.7 (1)
C16	0.6830 (3)	0.2423 (4)	0.2141 (2)	6.5 (1)
C17	0.5653 (3)	0.2216 (3)	0.2329 (2)	4.99 (7)
C21	0.2320 (3)	0.4071 (2)	0.4285 (1)	3.51 (6)
C22	0.3105 (3)	0.4138 (3)	0.4977 (2)	4.03 (6)
C23	0.4104 (3)	0.3372 (3)	0.5065 (2)	5.24 (8)
C24	0.4892 (4)	0.3449 (4)	0.5694 (2)	6.26 (9)
C25	0.4665 (4)	0.4272 (4)	0.6231 (2)	6.59 (9)
C26	0.3677 (4)	0.5028 (4)	0.6148 (2)	6.52 (9)
C27	0.2887 (3)	0.4960 (3)	0.5522 (2)	5.45 (8)
C31	0.5002 (4)	0.2734 (4)	0.0090 (2)	7.5 (1)
C32	0.3818 (3)	0.3123 (3)	0.0315 (2)	4.84 (7)
C33	0.2524 (5)	0.4856 (4)	0.0480 (3)	11.3 (1)
C34	0.1645 (6)	0.4721 (8)	−0.0126 (4)	18.1 (3)

the data for $VOCl(bz)_2$ and VO(OiPr)L (n = 5) yielded 2795 and 1489 independent reflections, respectively, for which $I > 3\sigma$.

The atom-labeling schemes for $VOCl(bz)_2$ and VO(OiPr)L (n = 5) are shown in Figures 2 and 3, respectively. Figure 3 shows half of the centrosymmetric VO(OiPr)L (n = 5) dimer; the other half is related by inversion, with C6 bonded to C7′ and C7 bonded to C6′. Positional and thermal parameters obtained for $VOCl(bz)_2$ in the final least-squares cycle are given in Table III. The final weighted and unweighted R factors were 4.76 and 3.43%, respectively. Positional and thermal parameters for VO(OiPr)L (n = 5) are shown in Table IV. The final weighted and unweighted R's were 6.19 and 5.05%, respectively.

Results and Discussion

Structure and Analyses. The two analyses reported here represent the first structural characterization of any vanadium hydroxamate complex. Figures 4 and 5 show stereoviews of $VOCl(bz)_2$ and VO(OiPr)L (n = 5), respectively. Both complexes have distorted octahedral coordination around the vanadium. In both, the oxo group is cis to the other monodentate ligand and trans to the carbonyl oxygens in the hydroxamate moieties. This is similar to what is seen for the related molybdenum complexes: MoO_2(hydroxamate)$_2$ with hydroxamates N-hydroxyphenacetin, N-hydroxyacetanilide, or benzohydroxamate, in which the two oxo ligands are cis to each other and trans to the carbonyl oxygens of the hydroxamate.[25,26] It is also similar to the structure of VO_2^+ chelates[27] and to oxoaquobis(oxalato)vanadium(IV) $[VO(H_2O)(ox)_2]$[28] and oxoisopropoxobis(8-hydroxyquinolinato)vanadium(V) $[VO(OiPr)(8hq)_2]$.[29]

Table IV. Positional Parameters and Anisotropic Thermal Parameters for $[VO(OiPr)L]_2$

atom	x	y	z	B_{eqv}, Å^2
V	0.0020 (1)	0.29317 (6)	−0.18808 (7)	4.20 (2)
O	0.0954 (5)	0.3571 (2)	−0.2415 (3)	4.8 (1)
O1	0.1222 (5)	0.3262 (2)	−0.0863 (3)	5.0 (1)
O2	−0.0953 (5)	0.2103 (3)	−0.0983 (2)	4.72 (9)
O3	−0.1678 (5)	−0.1968 (2)	0.1857 (3)	4.6 (1)
O4	0.1073 (5)	−0.2130 (2)	0.2673 (2)	4.48 (9)
O6	−0.1899 (5)	0.3496 (3)	−0.1942 (3)	4.9 (1)
N1	0.0957 (7)	0.2825 (4)	−0.0156 (3)	6.3 (2)
N2	0.0372 (6)	−0.1339 (3)	0.2630 (3)	4.4 (1)
C1	0.268 (1)	0.3812 (6)	0.0676 (5)	9.4 (2)
C2	0.231 (1)	0.2886 (6)	0.0523 (5)	8.6 (2)
C3	0.372 (1)	0.2365 (7)	0.0274 (7)	11.9 (3)
C4	−0.0216 (8)	0.2204 (4)	−0.0294 (4)	5.5 (2)
C5	−0.055 (1)	0.1663 (5)	0.0455 (5)	7.1 (2)
C6	−0.2095 (9)	0.1118 (5)	0.0210 (5)	6.7 (2)
C7	−0.263 (1)	0.0654 (5)	0.0955 (5)	7.5 (2)
C8	−0.1547 (9)	−0.0056 (4)	0.1232 (4)	6.5 (2)
C9	−0.2035 (9)	−0.0479 (4)	0.2023 (4)	5.7 (2)
C10	−0.1069 (7)	−0.1290 (4)	0.2192 (4)	4.2 (1)
C11	0.1455 (9)	−0.0650 (4)	0.2962 (4)	5.8 (2)
C12	0.208 (1)	−0.0816 (6)	0.3882 (5)	9.3 (3)
C13	0.286 (1)	−0.0580 (5)	0.2458 (5)	8.2 (2)
C14	−0.347 (1)	0.3264 (5)	−0.1711 (5)	7.9 (2)
C15	−0.473 (1)	0.3156 (6)	−0.2482 (6)	9.4 (3)
C16	−0.405 (1)	0.3949 (8)	−0.1169 (6)	11.1 (3)

All of the above-mentioned compounds exhibit what is commonly known as either the "trans influence" or "structural trans effect". In the kinetic trans effect as first observed in square-planar platinum complexes,[30,31] certain ligands trans to a negatively charged ligand are found to have faster exchange rates than those cis to the same ligand. A weakening (lengthening) of the trans bond compared to cis is also observed and is called the structural trans effect and is also seen in many octahedral complexes. Various theoretical models[32-34] all agree in predicting that a strongly bound ligand will preferentially weaken other ligand bonds in the trans position. Thus, ligands that tend to form strong bonds will preferentially form cis geometric isomers.

The complex VO(OiPr)L (n = 5) is dimeric, which is consistent with the molecular weight data discussed below. The dimer is a centrosymmetric molecule in which each ligand is bound in a bridging position between the two vanadium atoms.

Tables V and VI show the bond lengths and angles in each structure. The V=O bond is 1.599 (1) Å in $VOCl(bz)_2$ and 1.591 (3) Å in VO(OiPr)L (n = 5), within the range 1.52–1.68 Å

(25) Brewer, G. A.; Sinn, E. *Inorg. Chem.* **1981**, *20*, 1823–1830.
(26) Wieghardt, K.; Holzbach, W.; Hofer, E.; Weiss, J. *Inorg. Chem.* **1981**, *20*, 343–348.
(27) (a) Scheidt, W. R.; Tsai, C.-C.; Hoard, J. L. *J. Am. Chem. Soc.* **1971**, *93*, 3867–3872. (b) Scheidt, W. R.; Collins, D. M.; Hoard, J. L. *J. Am. Chem. Soc.* **1971**, *93*, 3873–3877. (c) Scheidt, W. R.; Collins, D. M.; Hoard, J. L. *J. Am. Chem. Soc.* **1971**, *93*, 3878–3882.
(28) Oughtred, R. E.; Raper, E. S.; Shearer, H. M. M. *Acta Crystallogr., Sect. B* **1976**, *B32*, 82–87.
(29) Scheidt, W. R. *Inorg. Chem.* **1973**, *12*, 1758–1761.
(30) Chernyaev, I. I. *Izv. Inst. Izuch. Platiny Drugikh Blagorodn. Met., Akad. Nauk SSSR* **1926**, *4*, 243–261.
(31) Basolo, F.; Pearson, R. *Mechanisms of Inorganic Reactions*; Wiley: NY, 1967.
(32) Basolo, F.; Pearson, R. G. *Prog. Inorg. Chem.* **1962**, *4*, 416–453.
(33) Butcher, R. J.; Penfold, B. R.; Sinn, E. *J. Chem. Soc., Dalton Trans.* **1979**, 668–675.
(34) Burdett, J. K.; Albright, T. A. *Inorg. Chem.* **1979**, *18*, 2112–2120.

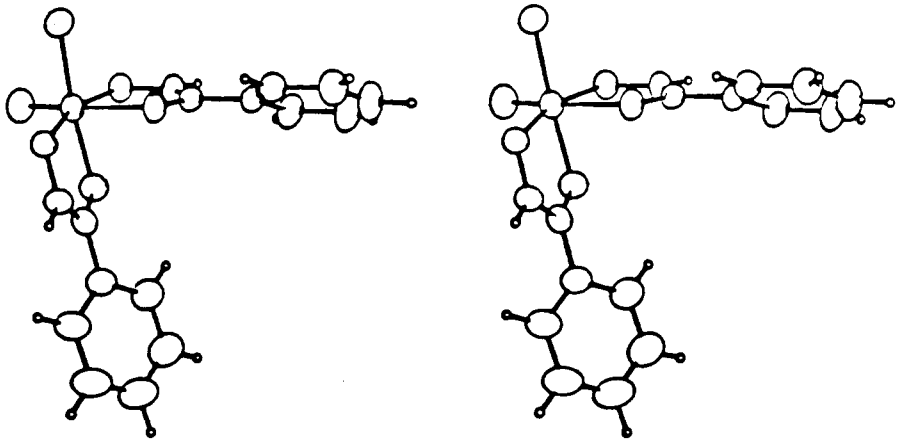

Figure 4. Stereoview of the $VOCl(bz)_2$ molecule.

Table V. Intramolecular Distances (Å) and Angles (deg) for $VOCl(bz)_2$

	Distances		
V–Cl	2.277 (1)	C12–C13	1.384 (3)
V–O	1.599 (1)	C13–C14	1.393 (3)
V–O11	1.852 (1)	C14–C15	1.381 (4)
V–O21	1.953 (1)	C15–C16	1.377 (4)
V–O12	2.193 (1)	C16–C17	1.398 (3)
V–O22	2.011 (1)	C17–C12	1.385 (3)
C11–O12	1.237 (2)	C22–C23	1.385 (3)
C21–O22	1.272 (2)	C23–C24	1.389 (4)
N1–O11	1.347 (2)	C24–C25	1.369 (4)
N2–O21	1.379 (2)	C25–C26	1.368 (4)
N1–C11	1.339 (2)	C26–C27	1.387 (4)
N2–C21	1.298 (2)	C27–C22	1.377 (3)
C11–C12	1.481 (3)	C31–C32	1.474 (4)
C21–C22	1.479 (3)	C32–O31	1.202 (3)
		C32–O32	1.318 (3)
		O32–C33	1.496 (4)
		C33–C34	1.422 (8)
	Angles		
O–V–Cl	99.00 (6)	C17–C12–C13	120.89 (20)
O–V–O11	93.23 (7)	C12–C13–C14	119.73 (22)
O–V–O21	105.56 (7)	C13–C14–C15	119.4 (3)
O–V–O22	98.58 (8)	C14–C15–C16	120.88 (23)
O–V–O12	168.97 (7)	C15–C16–C17	120.1 (3)
Cl–V–O11	102.76 (5)	C16–C17–C12	118.96 (24)
Cl–V–O12	84.43 (4)	V–O21–N2	113.21 (10)
Cl–V–O21	84.71 (4)	V–O22–C21	114.74 (13)
Cl–V–O22	158.08 (4)	O21–N2–C21	116.09 (16)
O11–V–O12	75.77 (5)	N2–C21–O22	117.59 (19)
O11–V–O21	158.56 (6)	O22–C21–C22	122.26 (18)
O11–V–O22	89.21 (6)	N2–C21–C22	120.14 (19)
O12–V–O21	85.14 (5)	C21–C22–C23	118.57 (21)
O12–V–O22	80.77 (6)	C21–C22–C27	121.87 (21)
O21–V–O22	78.03 (5)	C27–C22–C23	119.53 (22)
V–O11–N1	119.37 (10)	C22–C23–C24	120.17 (25)
V–O12–C11	111.00 (12)	C23–C24–C25	119.7 (3)
O11–N1–C11	116.04 (15)	C24–C25–C26	120.5 (3)
N1–C11–O12	117.22 (18)	C25–C26–C27	120.3 (3)
O12–C11–C12	123.48 (18)	C26–C27–C22	119.9 (3)
N1–C11–C12	119.30 (18)	C31–C32–O31	126.42 (24)
C11–C12–C13	117.02 (19)	C31–C32–O32	111.5 (3)
C11–C12–C17	122.07 (19)	O31–O32–O32	122.05 (24)
		C32–O32–C33	117.13 (23)
		O32–C33–C34	103.5 (5)

observed for vanadyl V=O bonds. The V–Cl bond length is 2.277 (1) Å, very close to the averages observed in the complexes $VOCl_3$(benzonitrile) and $VOCl_3$(benzonitrile)$_2$ [2.228 (3) and 2.269 Å, respectively[35]]. The V–O bond involving the isopropoxo group is 1.803 Å, significantly shorter than the predicted V–O bond length of 1.99 Å (from the sum of the ionic radii)[36] or 1.93 Å (predicted on the basis of vanadate structures[37]) and is almost as short as the 1.774 (2)-Å bond involving the isopropoxo group in VO(OiPr)(8hq)$_2$.[29] The shortening of this bond indicates some multiple-bond character.[23]

The O–V–Cl bond angle is 99.00 (6)°, and the O–V–OiPr bond angle is 97.9 (2)°. For the complexes $VO(H_2O)(ox)_2$, VO(OiPr)L (n = 5), VO(OiPr)(8hq)$_2$, and $VO_2(ox)_2$, there seems to be a

Table VI. Intramolecular Distances (Å) and Angles (deg) for $[VO(OiPr)L]_2$

	Distances		
V–O1	1.883 (3)	C1–C2	1.507 (10)
V–O4	1.939 (3)	C2–C3	1.518 (11)
V–O2	2.185 (3)	C4–C5	1.539 (8)
V–O3	2.040 (3)	C5–C6	1.543 (8)
V–O5	1.803 (3)	C6–C7	1.523 (8)
V–O	1.591 (3)	C7–C8	1.464 (8)
O1–N1	1.379 (5)	C8–C9	1.544 (7)
O4–N2	1.373 (5)	C9–C10	1.513 (7)
O2–C4	1.209 (6)	C12–C11	1.535 (8)
O3–C10	1.273 (6)	C11–C13	1.502 (8)
N1–C4	1.373 (6)	O5–C14	1.440 (7)
N2–C10	1.301 (6)	C14–C15	1.522 (9)
N1–C2	1.465 (7)	C14–C16	1.511 (10)
N2–C11	1.464 (6)		
	Angles		
O1–V–O2	77.18 (13)	O4–N2–C10	115.3 (4)
O3–V–O4	77.02 (14)	O4–N2–C11	115.3 (4)
O–V–O1	93.79 (16)	C10–N2–C11	128.5 (5)
O–V–O3	96.61 (15)	N1–C2–C1	107.6 (6)
O–V–O4	105.55 (16)	N1–C2–C3	107.2 (6)
O–V–O5	97.86 (16)	C1–C2–C3	115.4 (7)
O1–V–O3	85.29 (14)	N2–C11–C12	109.9 (5)
O1–V–O5	105.44 (16)	N2–C11–C13	109.1 (5)
O2–V–O3	80.92 (13)	C12–C11–C13	110.9 (5)
O2–V–O4	82.65 (13)	C4–C5–C6	109.4 (5)
O2–V–O5	86.53 (14)	C5–C6–C7	112.1 (5)
O4–V–O5	87.72 (15)	C6–C7–C8	112.8 (5)
O–V–O2	170.77 (15)	C7–C8–C9	112.0 (5)
O1–V–O4	155.01 (13)	C8–C9–C10	109.3 (4)
O3–V–O5	161.31 (14)	V–O5–C14	132.0 (3)
V–O1–N1	117.9 (3)	O5–C14–C15	110.5 (6)
V–O4–N2	113.9 (3)	O5–C14–C16	109.4 (6)
V–O2–C4	110.7 (3)	C15–C14–C16	109.0 (6)
V–O3–C10	113.3 (3)		
O1–N1–C4	113.9 (4)		
O1–N1–C2	113.9 (5)		
C2–N1–C4	128.2 (5)		

(35) (a) Gourdon, A.; Jeannin, Y. *Acta Crystallogr., Sect. B* **1980**, *B36*, 304–309. (b) Daran, J.-C.; Gourdon, A.; Jeannin, Y. *Acta Crystallogr., Sect B* **1980**, *B36*, 309–312.

(36) Ryan, R. R.; Mastin, S. H.; Reisfeld, M. J. *Acta Crystallogr., Sect B* **1971**, *B27*, 1270–1274.

(37) Bachmann, H. G.; Barnes, W. H. *Z. Kristallogr., Kristallgeom., Kristallphys., Kristallchem.* **1961**, *115*, 215.

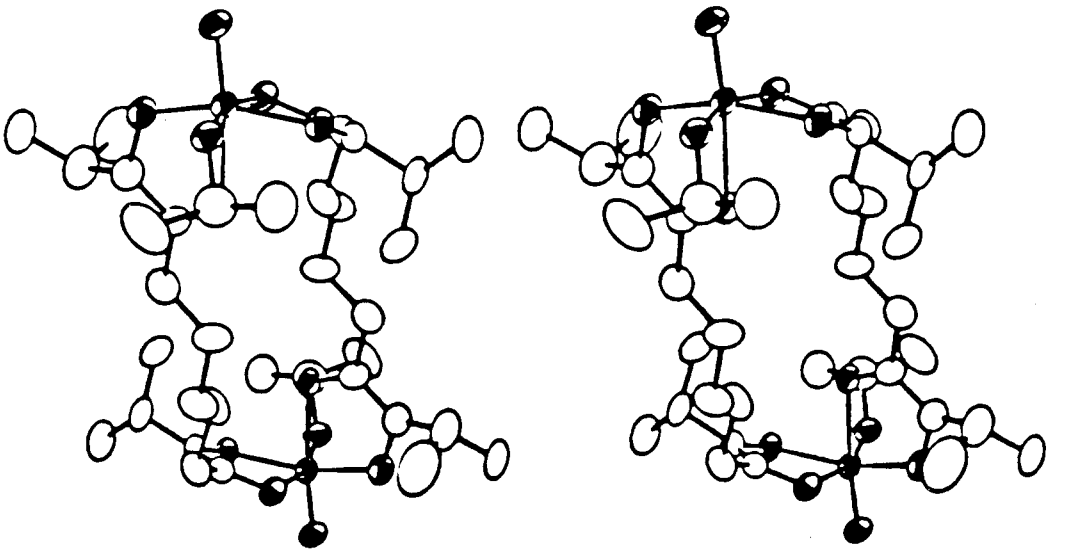

Figure 5. Stereoview of the VO(OiPr)L (n = 5) dimer. Darkened octants show vanadium and the six atoms in its coordination sphere.

correlation between the degree of double-bond character of the monodentate ligand cis to the oxo group and the size of the angle between these groups. The bond lengths involving the monodentate group cis to the oxo in the series above are 2.033 (3), 1.803 (3), 1.774 (2), and 1.648 (2) Å, while the bond angles are 95.5 (1), 97.9 (2), 101.9 (1), and 103.8 (1)°,[27-29] respectively. The shortening of the bond presumably increases the steric interference between the ligands, necessitating larger angles to relieve this strain.

In all of these structures the metal atom is displaced toward the oxo group, from the least-squares plane defined by the four ligating atoms cis to it. The displacement is 0.305 Å in $VOCl(bz)_2$ and 0.270 Å in VO(OiPr)L (n = 5), within the range 0.26–0.45 Å observed for other similar complexes.[27-29,35] In both structures there is also a smaller but significant displacement toward the other monodentate ligand [0.096 Å in $VOCl(bz)_2$ and 0.150 Å in VO(OiPr)L (n = 5)]. This displacement toward the second monodentate ligand once again seems to follow the double-bond character for the series $VO(H_2O)(ox)_2$, VO(OiPr)L (n = 5), $VO(OiPr)(8hq)_2$, and $VO_2(ox)_2$, with values of 0.030, 0.150, 0.220, and 0.26 Å, respectively.[27-29]

In both structures the bond trans to the oxo group is significantly lengthened, as is expected from the strong trans influence of the oxo group. In $VOCl(bz)_2$ this bond length is 2.193 (1) Å; in VO(OiPr)L (n = 5) it is 2.185 (3) Å. There is a smaller lengthening of the bonds opposite the chloro or isopropoxo ligands, which are 2.011 (1) and 2.040 (3) Å, respectively. In both structures, there is also a significant shortening of the V–O bonds, with the nitrogen-bound oxygen in the same chelate ring with the very elongated V–O bond. This phenomenon was also observed in the $VO(OiPr)(8hq)_2$ structure and may be due to the overall rigidity of the bond angles in the hydroxyquinoline ligands.[29] The bond angles in the hydroxamate chelate ring are also expected to be fairly rigid, due to the partial double-bond character of the C–N bond; however, the same phenomenon was not observed in $VO(H_2O)(ox)_2$.[28]

The ligand bite angles are 75.77 (5) and 78.03 (5)° in $VOCl(bz)_2$ and 77.2 (1) and 77.0 (1)° in VO(OiPr)L (n = 5). These angles are very similar to those of 75.1 (1)° and 81.3 (1)° found in $VO(H_2O)(ox)_2$, to those of 77.09 (9) and 76.27 (9)° in $VO(OiPr)(8hq)_2$, and to the angles in other oxovanadium chelate complexes.[27,29]

The bonds and angles within the ligands themselves are essentially the same as those found in the free ligands. The benzene rings of the benzohydroxamate are planar; the largest deviation from the least-squares planes is 0.008 Å for C14. There is also no significant variation of bond length or angle in the rings.

Spectroscopic and Physical Properties. Vanadium(V) Complexes. Complexes of stoichiometry and coordination sphere similar to those of VO(OiPr)L (n = 5) are formed with the n = 3, 5, and 10 ligands in either methanol or ethanol. Elemental analyses of the vanadium complexes are consistent with the stoichiometry VO(OR)L, where R = CH_3–, C_2H_5–, and $(CH_3)_2CH$–. The compounds are EPR silent, indicating that the vanadium has been oxidized from the +4 to the +5 state upon complexation by the hydroxamate group. The compounds with n = 5 and 10 are very soluble in $CHCl_3$ and CH_2Cl_2. However, in the absence of alcohols they decompose slowly in these solvents. The n = 3 complexes are only sparingly soluble, indicating that they are probably associated in the solid state. In addition to forming the X-ray-quality crystals discussed above from 2-propanol, the n = 5 complex formed needles from methanol and diamond-shaped plates from ethanol. The crystals of the methoxo and ethoxo complexes were not of X-ray quality.

The solid-state infrared spectra of the complexes with n = 3, 5, and 10 are essentially superimposable, with ν(V=O) of 953–958 cm^{-1}. In the methoxo compounds ν(C–H, OCH_3) at 2800 cm^{-1} is well-separated from the other aliphatic C–H stretching modes. They exhibit an additional band at 2900 cm^{-1} (shoulder), which may be assigned as the asymmetric C–H stretch of the methoxo group.

The visible spectra of the methoxo complexes were measured in 50% $CHCl_3/CH_3OH$ and are all superimposable with a broad asymmetric band at λ_{max} = 446 nm (ϵ = 3020–3340 M^{-1} cm^{-1}) and a shoulder on a large UV band at λ_{max} = 272 nm (ϵ = 3500–3700 M^{-1} cm^{-1}). Since V(V) has a d^0 electronic configuration, these bands must be charge-transfer in nature.

The visible and infrared spectra of these compounds indicate that they form complexes whose vanadium(V) coordination environments are very similar to that of the n = 5 isopropoxo complex, whose crystal structure is discussed above. Molecular weight measurements in 1:1 $CHCl_3/CH_3OH$ (using gel partition chromatography) suggest that both the n = 3 and 5 methoxo complexes are dimeric in solution (like the n = 5 isopropoxo complex), whereas the n = 10 methoxo complex appears to be monomeric. Figure 6 shows the elution volume plotted versus log MW for these compounds. The column was standardized by using the monomeric iron complex tris(benzohydroxamato)Fe(III) and the dimeric iron complex, methoxy-bridged n = 5 dimer, $[FeL(OCH_3)]_2$ (n = 5). Good agreement with the calibration curve was obtained only for the n = 10 monomer and n = 3 and 5 dimers of the vanadium complexes. However, the low solubility of the n = 3 complex suggests that it may be more highly associated in the solid state.

As mentioned earlier, it has been proposed[11] that an electron-withdrawing group on the hydroxamato nitrogen substituent is necessary in order for the oxoalkoxovanadium(V) complexes to be stable in the solid state. Ghosh and Sarkar[12,13] have recrys-

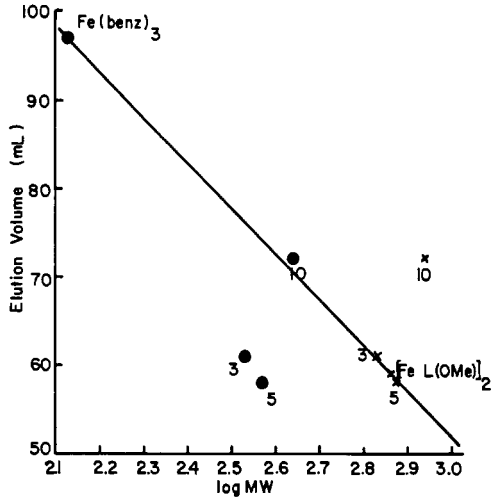

Figure 6. Elution volume vs log MW plotted for oxomethoxovanadium(V) complexes. Points are plotted for both monomeric (●) and dimeric (×) formulations of the complexes.

tallized the oxohydroxovanadium(V) complexes of adipo- and pimelohydroxamic acids from ethanol and acetone/ethanol, respectively, and the alkoxo complexes were not formed. The fact that the dihydroxamate ligands with the more electron-rich isopropyl substituent *do* form alkoxo complexes suggests that it is not necessary for the nitrogen substituent to be electron withdrawing for the alkoxo complexes to be stable in the solid state.

Vanadium(IV) Complexes. As described in the Experimental Section, preparations of oxovanadium(IV) rhodotorulate used both aqueous $VOSO_4$ and methanolic $VO(acac)_2$. In both cases (1:1) solutions of H_2RA and oxovanadium(IV) yielded a pale violet powder that was identified by elemental analysis and the IR spectra as oxovanadium(IV) rhodotorulate, VO(RA).

In contrast, when a methanolic solution of $VOSO_4$ and H_2RA (1:1) was prepared by using inert-atmosphere techniques, no VO(RA) was obtained.[38] Instead, as the ligand and metal each dissolved, a burgundy red color was observed. The UV/vis spectrum (λ_{max} = 390 and 516 nm, $\epsilon \geq 10^3$ M^{-1} cm^{-1}) indicated the presence of a species that was different from either the vanadium(IV) VO(RA) or the vanadium(V) $VO(RA)(OCH_3)$. EPR measurements subsequently confirmed that the predominant species in this solution was a vanadium(IV) complex (≥70% vanadium(IV) on the basis of a comparison with a $VO(acac)_2$ standard). Cyclic voltammograms of DMSO solutions of $VOSO_4$ and H_2RA (1:1 and 1:3) and of the red VO(RA) exhibited $V^{IV/III}$ couples at 0.069, 0.044, and 0.041 V vs the $Ag/AgNO_3$ reference for each of the samples. The couples observed for the (1:1) solution of VO(RA) + H_2RA and for that of $VO(RA)(OCH_3)$ were irreversible, while that for the (3:1) solution of metal and ligand was quasi-reversible. The 1:1 VO/RA system in aqueous solution showed a redox potential of 0.51 V vs NHE, which was essentially independent of pH from pH 4 to 7. Below pH 4 the potential increased by about 0.06 V/pH unit, consistent with a single proton stoichiometry and the electrode reaction

$$VO(RA)(OH) + H^+ + e^- = VO(RA) + H_2O$$

These results indicate that the hydroxamate chelating group is capable of displacing the vanadyl oxygen to form a tris(hydroxamato)vanadium(IV) complex of rhodotorulic acid. In the only known example of such a reaction in protic solvents, catecholate ligands have been shown to be able to form both the bis(catecholato)oxovanadate(IV) and the tris(catecholato)vanadate(IV).[39] These complexes, which have been isolated and characterized by X-ray crystallography, exhibit some physical properties that are quite similar to those reported here for their rhodotorulate analogues. The electronic spectrum of the bis(catecholato)oxovanadate(IV) complex is characterized by weak d–d transitions ($\epsilon < 100$ M^{-1} cm^{-1}), but the tris(catecholato)vanadate(IV) complex exhibits only intense charge-transfer transitions ($\epsilon \geq 9 \times 10^3$ M^{-1} cm^{-1}). In addition, the observed $V^{IV/III}$ couple of bis(catecholato)oxovanadate(IV) is irreversible, whereas that of the tris(catecholato)vanadate(IV) complex is quasi-reversible.[39] Since oxovanadium(IV) complexes typically exhibit irreversible cyclic voltammetric reductions due to the loss of the oxygen atom immediately following the $V^{IV/III}$ reduction, observation of a reversible or quasi-reversible couple is strong evidence for replacement of the vanadyl oxygen by the chelating ligand.

Attempts to isolate the proposed tris(dihydroxamato)divanadium(IV) complex were based on an assumed formulation of $[V_2(RA)_3]^{2+}$, deemed the most likely on the basis of its similarity to the known stoichiometry of the Fe^{3+} complex, $Fe_2(RA)_3$.[40] An excess of ligand was used along with tetraphenylborate to precipitate the crude, dark red-violet product. This approach was used with a similar result by using the $n = 3$ dihydroxamate ligand. Physical characterization of the resultant red powders obtained in this way was consistent with the displacement of the vanadyl oxygen by ligand. Although the pale violet powder, VO(RA), exhibits a strong absorbance in its infrared spectrum at ~970 cm^{-1} (assigned as the V=O stretch), this band is absent in the red tris(dihydroxamato)divanadium(IV) products. The burgundy red methanolic solution of the vanadium(IV) tris(hydroxamate) rhodotorulate complex, when exposed to air, gradually changed to that (λ_{max} ~ 446 nm, ϵ ~ 3100 M^{-1} cm^{-1}) of $VO(RA)(OCH_3)$, the expected vanadium(V) oxidation product (Figure S2).[23] A comparison of the spectra of the vanadium(IV) and -(V) complexes of RA and the $n = 3$ dimer is presented in Table VII. A recent report of complex formation between the trihydroxamic acid ligand desferrioxamine B and vanadium(V) has appeared.[4] No isolation or characterization of the complex was reported, other than to show a 1:1 metal:ligand ratio. The vis/UV spectra reported seem to be more characteristic of vanadium(IV) than -(V).

Table VII. Electronic Spectral Data for Vanadium(IV) and -V Rhodotorulate and Synthetic Dihydroxamate Complexes

complex	solvent	abs max,[a] nm ($10^{-3}\epsilon$, M^{-1} cm^{-1})
	Vanadium(IV) Complexes	
$[V_2(RA)_3]^{2+}$ [b]	H_2O	390 sh, 516
$[V_2(RA)_3]^{2+}$ [b]	CH_3OH	390 (≥3.3), 516 (≥2.4)
$[V_2L_3]^{2+}$ [b]	CH_3OH	385 (≥3), 516 (≥3)
$[V_2L_3]^{2+}$ [b]	CH_3CN	381, 505
	Vanadium(V) Complexes	
VO(RA)(OH)	H_2O	289 (3.7), 464 (2.2), 556 (2.3)
$VO(RA)(OCH_3)$	CH_3OH	432 (2.3)
$VOL(OCH_3)$ [c]	CH_3OH	272 (3.6), 446 (3.2)
$VOL(OCH_3)$ [c]	CH_3CN	294, 440, 544

[a] In those cases where extinction coefficients are not reported, the solution concentrations could not be quantitatively determined. [b] Proposed stoichiometry; see text. [c] L = *N,N'*-dihydroxy-*N,N'*-diisopropylheptanediamide.

Summary

Vanadium hydroxamate complexes that are relevant to widely used analytical procedures have been characterized. The first X-ray crystallographic structures of any vanadium hydroxamates are reported. In the vanadium(V) and vanadyl complexes, the vanadium is found in a distorted octahedral environment in which a pronounced structural trans effect can be observed. The characterization of several vanadium(IV) hydroxamate complexes has been accomplished and evidence for a tris(hydroxamato)va-

(38) This section reports the initial experiment whereby it was discovered that a tris(hydroxamato)vanadium(IV) complex was being formed. For that reason, the subsequent synthesis of this compound uses a 2:1 ligand to metal ratio rather than the 1:1 ratio used in the initial experiment.

(39) Cooper, S. R.; Koh, Y. B.; Raymond, K. N. *J. Am. Chem. Soc.* **1982**, *104*, 5092–5102.

(40) Carrano, C. J.; Cooper, S. R.; Raymond, K. N. *J. Am. Chem. Soc.* **1979**, *101*, 599–604.

(41) Batinic, I.; Birus, M.; Pribanic, M. *Croat. Chem. Acta* **1987**, *60*, 279–284.

nadium(IV) complex has been found. Hydroxamate and catecholate ligands are unique to date in being able to break the strong V=O vanadyl bond in an aqueous environment.

Acknowledgment. This research was supported by NIH Grant AI 11744.

Registry No. $(VO(OCH_3)L)_2$ (n = 3), 123264-09-5; $(VO(OC_2H_5)L)_2$ (n = 3), 123264-10-8; $(VO(OCH_3)L)_2$ (n = 5), 123264-11-9; $(VO(OC_2H_5)L)_2$ (n = 5), 123264-12-0; $VO(OCH_3)L$ (n = 10), 123264-13-1; $VOCl(bz)_2$, 123264-15-3; $(VO(OiPr)L)_2$ (n = 5), 123264-16-4; $VO(acac)_2$, 3153-26-2; $VO(RA)(OCH_3)$, 123264-18-6; $VO(RA)\cdot H_2O$, 123264-19-7; $[V_2(RA)_3]^{2+}$, 123264-17-5; oxovanadium(IV) sulfate, 27774-13-6.

Supplementary Material Available: Figures S1 and S2, showing vis/UV spectra of vanadium(IV/V) rhodotorulate complexes from spectroelectrochemical experiments and vis/UV spectra of a vanadium(IV) rhodotorulate complex in solution upon exposure to air, and Tables S1, S4, and S5, listing crystallographic summary data and anisotropic thermal parameters for $VOCl(bz)_2$ and $[VO(OiPr)L]_2$ (n = 5) (6 pages); Tables S2 and S3, listing calculated and observed structure factors for $VOCl(bz)_2$ and $[VO(OiPr)L]_2$ (n = 5) (39 pages). Ordering information is given on any current masthead page.

Contribution from the Departments of Chemistry, University of Missouri—Rolla, Rolla, Missouri 65401, and Abilene Christian University, Abilene, Texas 79699, Nuclear Physics Division, Atomic Energy Research Establishment, Harwell, Didcot OX11 0RA, England, and Institut de Physique, Universite de Liege, B-4000 Sart Tilman, Belgium

Study of the High-Temperature Spin-State Crossover in the Iron(II) Pyrazolylborate Complex $Fe[HB(pz)_3]_2$

Fernande Grandjean, Gary J. Long,* Bennett B. Hutchinson,* LaNelle Ohlhausen, Paul Neill, and J. David Holcomb

Received January 6, 1989

A study of the infrared and Mössbauer spectra and magnetic properties of $Fe[HB(pz)_3]_2$ indicate that this nominally low-spin iron(II) compound undergoes a spin-state crossover to the high-spin state accompanied by a crystallographic phase change at about 400 K. The crystallographic phase transition shatters the crystals and leads to a large hysteresis in the magnetic moment upon cooling from 460 to about 250 K. The analyses of the Mössbauer spectra, obtained as a function of temperature during both heating and cooling, indicate the presence of spin-state relaxation on the Mössbauer time scale of 10^{-8} s. The activation energy for this relaxation process is 7300 cm^{-1} for freshly sublimed $Fe[HB(pz)_3]_2$ and 1760 cm^{-1} after the crystals have undergone the phase transition. Both the magnetic moments and Mössbauer spectra indicate that between 295 and 430 K the ground state of $Fe[HB(pz)_3]_2$ has a temperature-dependent population of both the high-spin and low-spin electronic configurations. The optical absorption spectrum provides further support for the spin-state crossover and DSC and volume expansion studies indicate the presence of the phase transition at the spin-crossover. Analysis of the far-infrared spectrum utilizing $^{54}Fe/^{57}Fe$ substitution at both room and high temperatures allows unambiguous assignment of the Fe–N stretching bands both in high-spin and low-spin forms. The low-spin Fe–N stretching bands appear at 459, 434.5, and 399.5 cm^{-1}, whereas upon heating the high-spin Fe-N stretching bands appear at 257.5 and 223 cm^{-1}. Measurement of the area of these bands as the temperature is increased reflects the change in the population of the low-spin and high-spin states.

Introduction

In 1931 Cambi and co-workers found an anomalous, temperature-dependent, magnetic behavior for several Fe(dialkyldithiocarbamate)$_3$ complexes.[1] Their investigation revealed a behavior which they attributed to a rearrangement of the electrons in the d orbitals as the temperature was decreased below room temperature. Twenty-five years later, Maki[2] and Ballhausen[3] applied crystal field theory to these and similar compounds, and attributed the magnetic behavior to a change from a high-spin, weak-field electronic configuration to a low-spin, strong-field configuration. Now transition-metal complexes with a variety of metals, oxidation states, and ligands, have been observed to change their spin-state and exhibit spin-crossover phenomena. First-row transition-metal complexes with $3d^4$ to $3d^7$ electronic configurations have been found to change between a high-spin and a low-spin configuration,[4] but iron complexes are the most abundant as indicated in various reviews.[5-9] The spin-crossover in these complexes may occur with changes in temperature, pressure,[10-12] and coordination number and with exposure to light.[13,14]

Additional interest in these compounds has been created by the recognition that, in some biologically significant molecules, spin-state change is an important part of their reaction mechanism.[15-17]

The tris(1-pyrazolyl)borate ligand, $HB(pz)_3^-$, and its methyl-substituted derivatives produce a ligand field in which iron(II) compounds may form either the high-spin or low-spin state or make both states thermally accessible. Trofimenko and his coworkers initiated the study of these systems by using a variety of techniques.[18] Thermochromic changes in solid $Fe[HB(pz)_3]_2$ led to the initial proposal that this complex undergoes a change in spin state upon heating.[19] Confirmation of this change was demonstrated by the large increase in its magnetic moment upon heating to ca. 400 K.[20] The room-temperature far-infrared

* Address correspondence to these authors at the University of Missouri—Rolla for G.J.L. and Abilene Christian University for B.B.H.

(1) Cambi, L.; Cagnasso, A. *Atti, Accad. Naz. Lincei, Cl. Sci. Fis. Mat. Natl., Rend.* **1931**, *13*, 809. Cambi, L.; Szego, L. *Ber. Dtsch. Chem. Ges. B* **1931**, *64*, 2591.
(2) Maki, G. *J. Chem. Phys.* **1958**, *28*, 651-662.
(3) Ballhausen, C. J.; Liehr, A. D. *J. Am. Chem. Soc.* **1959**, *81*, 538-542.
(4) Martin, R. L.; White, A. H. In *Transition Metal Chemistry*; Carlin, R. L., Ed.; Decker: New York, 1968; Vol. 4, pp 113-198.
(5) Gütlich, P. In *Mössbauer Spectroscopy Applied to Inorganic Chemistry*, Long, G. J., Ed.; Plenum: New York, 1984; Vol. 1, pp 287-337.
(6) Goodwin, H. A. *Coord. Chem. Rev.* **1976**, *18*, 293-325.
(7) Gütlich, P. *Struct. Bonding* **1981**, *44*, 83-202.
(8) König, E.; Ritter, G.; Kulshreshtha, S. K. *Chem. Rev.* **1985**, *85*, 219-234.
(9) König, E. *Prog. Inorg. Chem.* **1987**, *35*, 527-622.
(10) Pebler, J. *Inorg. Chem.* **1983**, *22*, 4125-4128.
(11) König, E.; Ritter, G.; Waigel, J.; Goodwin, H. A. *J. Chem. Phys.* **1985**, *83*, 3055-3061.
(12) Long, G. J.; Hutchinson, B. B. *Inorg. Chem.* **1987**, *26*, 608-613.
(13) Decurtins, S.; Gütlich, P.; Hasselbach, K. M.; Hauser, A.; Spiering, H. *Inorg. Chem.* **1985**, *24*, 2174-2178.
(14) Poganiuch, P.; Gütlich, P. *Inorg. Chem.* **1987**, *26*, 455-458.
(15) Gütlich, P. In *Chemical Mössbauer Spectroscopy*; Herber, R. H., Ed., Plenum: New York, 1984; pp 27-64.
(16) Wilson, D. F.; Dutton, P. L.; Erecinska, M.; Lindsay, J. G.; Sato, N. *Acc. Chem. Res.* **1972**, *5*, 234-241.
(17) Scheidt, W. R.; Reed, C. A. *Chem. Rev.* **1981**, *81*, 543-555.
(18) Jesson, J. P.; Trofimenko, S.; Eaton, D. R. *J. Am. Chem. Soc.* **1967**, *89*, 3158-3164.
(19) Jesson, J. P.; Weiher, J. F. *J. Chem. Phys.* **1967**, *46*, 1995-1996.
(20) Hutchinson, B.; Daniels, L.; Henderson, E.; Neill, P.; Long, G. J.; Becker, L. W. *J. Chem. Soc., Chem. Commun.* **1979**, 1003-1004.

0020-1669/89/1328-4406$01.50/0